# DISPLACEMENT OF MONOLITHIC RUBBLE-MOUND BREAKWATER CROWN-WALLS

Jørgen Quvang Harck Nørgaard[1], Lars Vabbersgaard Andersen[1], Thomas Lykke Andersen[1], and Hans F. Burcharth[1]

This paper evaluates the validity of a simple one-dimensional dynamic analysis as well as a Finite-Element model to determine the sliding of a rubble-mound breakwater crown-wall. The evaluation is based on a case example with real wave load time-series and displacements measured from two-dimensional physical model tests. The outcome is a more reliable evaluation of the applicability of simple dynamic calculations for the estimation of displacement of rubble-mound superstructures. The case example clearly demonstrates that a simplified one-dimensional sliding model provides a safe estimate of the accumulated sliding distance of crown-wall superstructures, which is in contrast to findings from previous similar studies on caisson breakwaters. The calculated sliding distance is approximately three times larger than the measured one when using the original one-dimensional model suggested in previous studies on caisson breakwaters, but correction terms are suggested in the present paper to obtain almost equal measured and estimated displacements. This is of great practical importance since many existing rubble-mound crown-walls are subjected to increasing wave loads due to rising sea water level from climate changes. Reliable and safe estimates are needed to determine whether displacements of crown wall superstructures during extreme situations would be acceptable or whether they lead to total failure of the structures.

*Keywords: rubble-mound breakwater; crown-wall; sliding; physical modeling; Finite-Element model*

## INTRODUCTION

### Presentation of the Problem

Several failure modes have to be considered when evaluating the stability of a crown-wall structure. The different failure modes are illustrated in Figure 1 where failure mode *a)* solely depends on the strength of the superstructure and the magnitude of the wave loads. Failure mode *b)* and *c)* are more complex since these also involve the properties of the soil and failure modes of other parts of the structure.

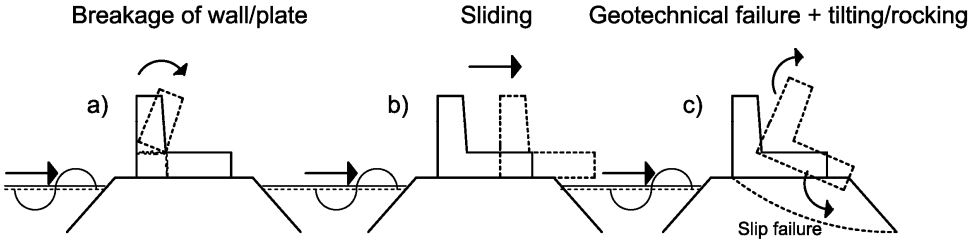


**Figure 1. Typical failure modes of crown-wall superstructures.**

The present paper is focusing on the failure modes b) and c) and is thereby assuming that the internal strength of the crown structure itself is sufficient to withstand the wave loads. The design against these failure modes is very complex due to both the complex dynamic loading and the dynamic response of the structure and soil. In many cases a quasi-static sliding and tilting criterion is used based on loadings estimated from hydraulic model tests or empirical formulae. However, due to the complexity of the material response, numerical solution methods must be applied to accurately determine the overall stability of such structures.

Crown wall superstructures are normally designed to remain fully stable during a specific extreme design sea state with a given return period. However, a structure designed for a sea state with e.g. a 100 year return period can still be exposed to e.g. a 1000 year wave condition during its lifetime. Moreover, existing structures can become unstable in the future due to climate changes leading to sea-water-level rise and thereby increasing wave loading. Thus, small displacements of the superstructures could be accepted, as the case for caisson breakwaters, instead of upgrading existing structures. However, in order to avoid total failures, a safe and rather accurate procedure is needed to estimate the actual displacements of the crown-walls.

[1] Department of Civil Engineering, Aalborg University, Sohngaardsholmsvej 57, DK-9000, Denmark, jhn@civil.aau.dk, la@civil.aau.dk, tla@civil.aau.dk, hansburcharth@gmail.com

### Existing Studies on Caisson Breakwaters

So far, there has not been much focus on the magnitude of the displacements of crown-walls, but several authors have evaluated the displacement of caisson breakwaters.

Burcharth et al. (2008) presented a comparison between sliding distances of a caisson breakwater estimated by a simple dynamic stability analysis and by a more sophisticated dynamic Finite-Element analysis. Simplified horizontal and vertical impulsive wave pressure distributions with different intensities and time variations were considered in the comparison. In the simple dynamic stability analysis the sliding along the interface between the structure and the breakwater was modelled according to Coulomb's friction law. The sliding velocity and the accumulated displacement of the structure were both obtained by integration of the equation of motion. The simple method neglected the elastic/plastic deformations of the foundation and the structure itself and the rotation of the structure.

Andersen et al. (2010) presented a series of numerical calculations based on the finite difference code FLAC in which the pore water elasticity and the drainage characteristics were included. Results from the FLAC model were further compared to results from a ABAQUS Finite-Element model where fully drained conditions were assumed. This was done to evaluate the influence of the pore pressures. Moreover, results from the two numerical models were compared to results from the simple dynamic stability analysis.

Burcharth et al. (2008) and Andersen et al. (2010) both concluded that the displacements of a relatively heavy weight caisson breakwater obtained from the simple one-dimensional analysis were on the unsafe side.

### Motivation of the Present Paper

For lighter structures with higher Eigen frequencies compared to caisson breakwaters, such as crown-walls, the analytical approach may lead to a different conclusion than found by Burcharth et al. (2008) and Andersen et al. (2010) since very large heal pressures generally does not exist for conventional crown-walls as for narrow and high caissons. A large heal pressure can lead to geotechnical slip failure in the foundation. The displacement hypothesis is illustrated in Figure 2.

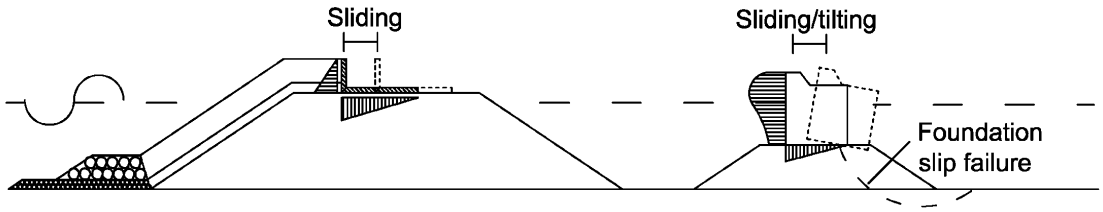


**Figure 2. Expected failure mode of a crown-wall super structure in contrast to the failure of a caisson breakwater.**

The remaining paper consists of three parts. First, a physical model test case study in scale 1:30 is described in which wave loads are measured on a static structure and the sliding displacement is measured on a moveable part of the crown-wall structure. Secondly, the sliding displacement of the crown-wall is estimated from a simple one-dimensional analysis and compared to the actual measured sliding displacement and to the estimated displacement from a more sophisticated Finite-Element model. In the last part a numerical study is performed in which scale effects related to the response in the underlying soil are evaluated. The evaluation in the second and third part is based on comparisons against measured displacements from the physical model tests in the first part.

The outcome of the paper is a more reliable evaluation of the applicability of simple dynamic calculations for the estimation of sliding distances of rubble-mound breakwater crown-walls.

## PHYSICAL MODEL TEST STUDY

Physical tests are performed in a 1.5 m wide and 25 m long wave flume at Aalborg University in scale app. 1:30, see Figure 3. The bottom in the flume is horizontal in the first 6.5 m followed by a 1:98 slope that continues until just before the model.

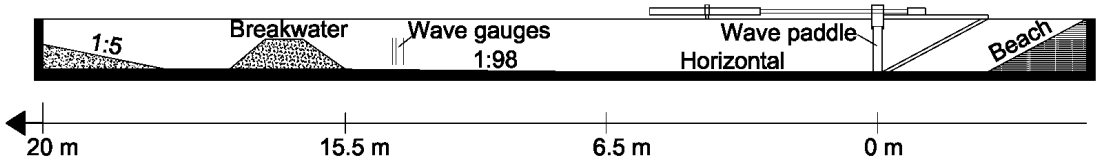


**Figure 3. Layout of model test in 2D wave flume.**

The tests are performed on a rubble-mound breakwater model with a typical crown structure. The dimensions of the model are shown in Figure 4.

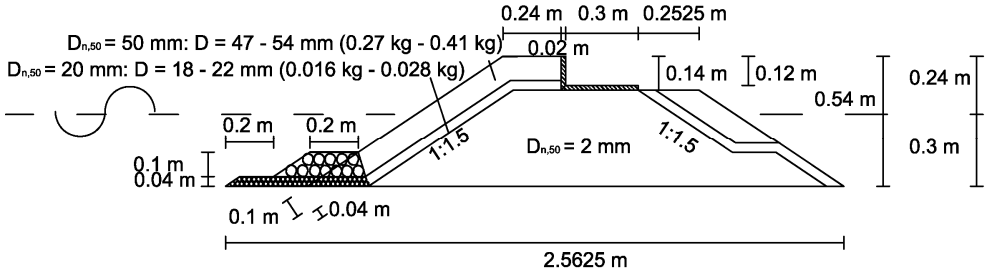


**Figure 4. Dimensions of the 1:30 scale model installed in the 2D wave flume.**

Wave pressures are measured under the base slap and on the vertical face using pressure transducers mounted directly on the superstructure. The vertical wave loads are subjected to scale effects due to flow not being fully turbulent in the model core material. An engineering compensation method is to increase the stone size in the core as proposed by Burcharth et al. (1999). Thus, the core material used in the laboratory model tests is slightly coarser than by Froude scaling. A small section of the superstructure is allowed to move freely during the tests to measure the actual displacements of the crown-wall. Regular waves are evaluated in the tests and wave conditions are changed in steps to obtain different displacements of the structure. Drück PMP UNIK series pressure transducers with a diameter of 20 mm are used for determining wave pressures on the fixed superstructure. The transducers are mounted flush with the structure wall face. The pressure sensors have a correct frequency response to 5 kHz and signals from the sensors are initially acquired and stored to the computer with 1.5 kHz. The pressure signals are hereafter filtered using a digital low-pass filter to obtain an appropriate cut-off corresponding to the spatial resolution of transducers. Based on the peak pressure celerities, the time-series for the horizontal wave forces are low-pass filtered to 250 Hz and the time-series for the vertical wave pressures are low-pass filtered to 100 Hz in order to avoid unrealistic peak pressures. The instrumentation of the superstructure is illustrated in detail in Figure 5. Pictures of the physical model test setup are given in Figure 6.

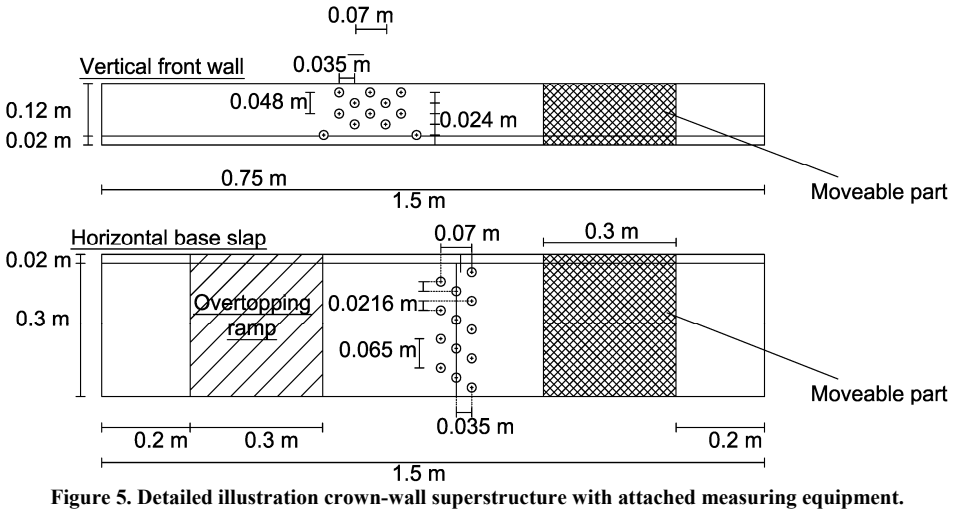


**Figure 5. Detailed illustration crown-wall superstructure with attached measuring equipment.**

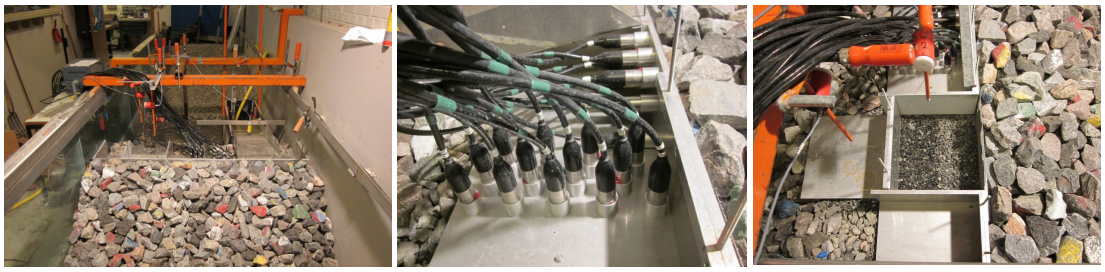

**Figure 6.** ***(left)*** **Front view of breakwater,** ***(middle)*** **Pressure transducers in static part of crown-wall,** ***(right)*** **Moveable part of crown-wall.**

### Integration of Wave Pressures

The wave induced forces and the related moments are determined by integration as explained in the following. The nomination of the pressures is shown in Figure 7.

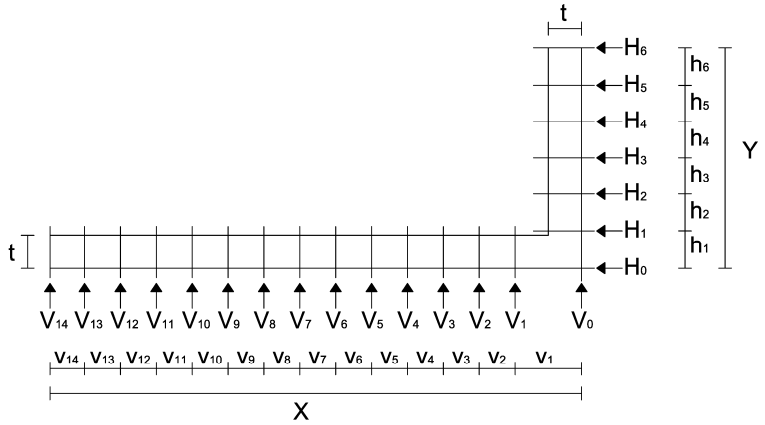


**Figure 7. Illustration of cross-sectional positioning of the pressure sensors on the crown-wall.**

$H_0$, $H_6$, $V_0$ and $V_{14}$ in Figure 7 are not measured directly but are estimated as described in the following.

- Pressure $H_0$ and $H_6$ at the bottom and top of the vertical face are obtained by linear extrapolation from $H_1$, $H_2$ and $H_4$, $H_5$, respectively. An example is given in Eq. 1 for calculation of $H_6$.
- Pressure $V_{14}$ at the rear corner of the deck plate is obtained by linear extrapolation from $V_{12}$ and $V_{13}$ using Eq. 2.
- V0 is set equal to $H_0$.

$$H_6 = H_5 - \frac{(H_4 - H_5)}{h_5} h_6 \tag{1}$$

$$V_{14} = V_{13} - \frac{(V_{12} - V_{13})}{v_{13}} v_{14} \tag{2}$$

The wave induced horizontal force $F_H$ and the corresponding moment around the toe of the vertical wall $M_{FH}$ are determined using Eq. 3.

$$\begin{aligned} \Delta F_{H,hn} &= \frac{1}{2} h_n \left( H_{n-1} + H_n \right) \\ F_H &= \sum_{n=1}^{n=6} \Delta F_{H,hn} \\ \Delta M_{F_{H,hn}} &= \frac{1}{2} h_n \left[ \sum_{i=1}^{n-1} (h_i)(H_{n-1} + H_n) + h_n \left( \frac{1}{3} H_{n-1} + \frac{2}{3} H_n \right) \right] \\ M_{F_H}^O &= \sum_{n=1}^{n=6} \Delta M_{F_{H,hn}} \end{aligned} \tag{3}$$

The wave induced vertical force $F_V$ and the corresponding moment around the rear corner of the horizontal deck plate $M_{FV}$ are determined using Eq. 4.

$$\Delta F_{V,vn} = \frac{1}{2} v_n \left( V_{n-1} + V_n \right)$$

$$F_V = \sum_{n=1}^{n=14} \Delta F_{V,vn}$$

$$\Delta M_{F_{V,vn}} = \frac{1}{2} h_n \left[ \sum_{i=1}^{n-1} \left( v_i \right) \left( V_{n-1} + V_n \right) + v_n \left( \frac{1}{3} V_{n-1} + \frac{2}{3} V_n \right) \right] \qquad (4)$$

$$M_{F_V}^O = \left( \sum_{i=1}^{i=14} v_i - \frac{\sum_{n=1}^{n=14} \Delta M_{F_{V,vn}}}{F_V} \right) F_V$$

An example of the integrated pressure distribution on the structure is given in Figure 8. Calculated forces and moments corresponding to the integrated pressure distribution are further given in the figure.

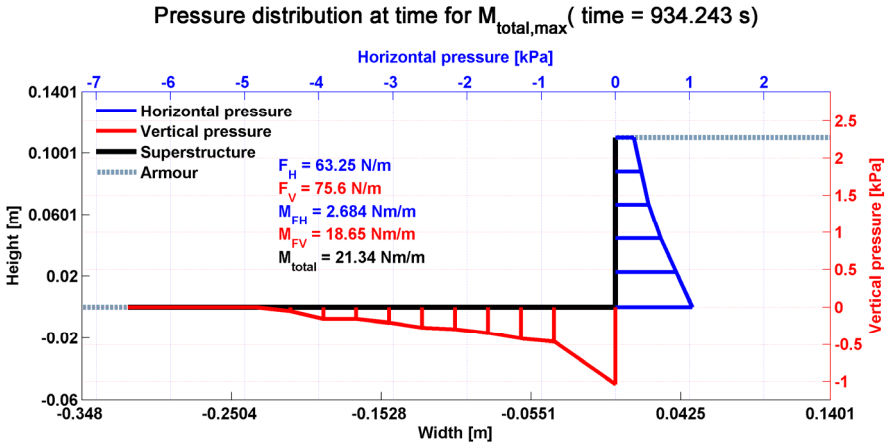


**Figure 8. Example of integrated wave induced pressure on superstructure at the instance of maximum total overturning moment.**

Another approach could be to fit a polynomial to the measured pressures in order to obtain a higher order extrapolation of the pressures at the bottom and top of the vertical face and at the front and rear corner of the deck plate. This would provide a more smooth pressure distribution than in Figure 8. However, the simple linear pressure extrapolation is still expected to provide a relatively good estimate of the overall horizontal and vertical forces and moments.

### Sliding of Moveable Section

Three potentiometers are used to measure the three degrees of freedom of the crown-wall, i.e. the horizontal movements, the vertical movements, and the overturning. The degrees of freedoms are determined based on the origin illustrated in Figure 9.

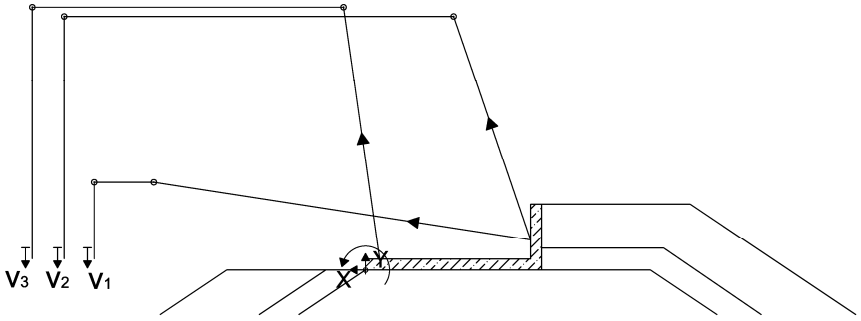

**Figure 9. Illustration of wires attached to the moveable section.**

A wire mesh is installed to avoid horizontal pressure from the amour units on the crown wall front. Moreover, low friction Teflon plates are installed on the interface with the fixed structure to guide the moveable part of the superstructure and to minimize friction. Sand is glued under the base of the superstructure to obtain a realistic friction of approximately $\mu \approx 0.6$ which is normal for prefabricated concrete crown-wall elements on quarry rock core material. The friction between the crown-wall and the core material is measured in wet conditions with all equipment attached. No noticeable difference is found between the static and dynamic coefficients which are both found to be approximately $\mu_s \approx \mu_d \approx 0.64$. The movements of the structure are sampled using the same frequency as for the pressure transducers, 1500 Hz.

### Considered Load Peak

Only a single wave condition is considered in the present paper based on regular waves with wave height $H = 0.161$ m, wave period $T = 2.2$ s, and water depth $h = 0.38$ m. Moreover, main focus is on the first wave load peak in the time-series to avoid influence from an initial displacement of the crown wall. The considered wave load peak is illustrated in Figure 10 where $F_H$ is the horizontal wave load and $F_V$ is the vertical wave load.

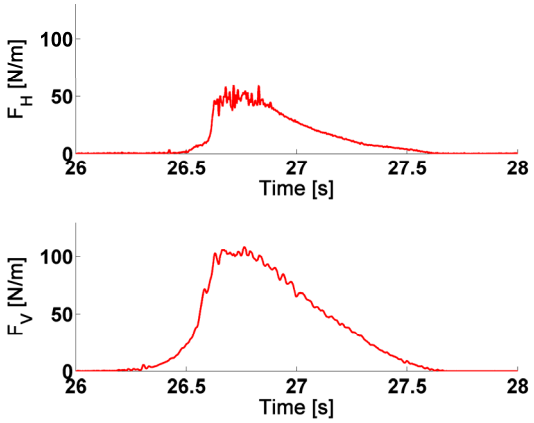


**Figure 10. Considered wave load peak measured on the static structure.**

The measured and interpolated wave pressure on the static superstructure is illustrated in Figure 11 at the instance of maximum total resulting wave load in the considered load peak. Additionally, the resulting horizontal and vertical attack points are illustrated in the figure. As seen, a relatively low horizontal attack point is obtained which is approximately corresponding to 1/3 of the wall height due to the approximately triangular pressure distribution. In contrast to caisson breakwaters the wave loads on crown-wall superstructures with rubble mound in front of the wall are not very impulsive due to the protective effect of the mound. The low resulting attack points leads to a higher stability of the structure against overturning compared to caisson breakwaters and it is therefore also expected that the displacement failure mechanism for the crown-wall will be sliding.

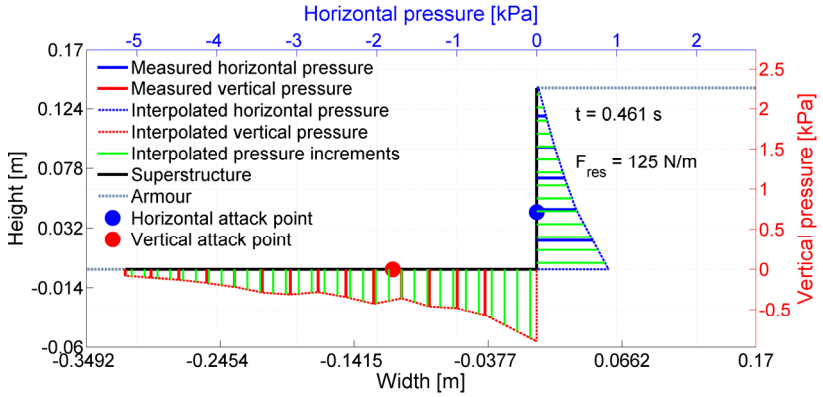


**Figure 11. Measured and interpolated pressure on static structure at instance of maximum resulting total wave load.**

It should be mentioned, that regular waves are considered in the present study. Irregular waves may lead to more impulsive horizontal wave loads on the structure. Moreover, if a part of the wall is left un-protected the resulting horizontal force attack point is expected to be higher. Impulsive horizontal loads are, however, not peaking at the same time instance as the vertical load.

## EVALUATION OF SIMPLIFIED SLIDING MODEL

The sliding along the interface between the structure and the breakwater is modelled according to Coulomb's friction law, as proposed by Burcharth et al. (2008). The one-dimensional approach neglects elastic/plastic deformations in the foundation and the structure itself. Moreover, the rotation of the structure is disregarded. The sliding displacement in the positive x-direction is determined from the equation of motion:

$$F(t) = \left(M_{structure} + M_{added}\right)\frac{d^2x}{dt^2} = -\left(G - F_V(t)\right)\mu + F_H(t) = -g \qquad (5)$$

where $F(t)$ is the reduced force time-series [N], $F_H(t)$ is the horizontal force time-series [N], $F_V(t)$ is the vertical force time-series [N], $M_{structure}$ is the mass of the structure reduced for buoyancy [kg], $M_{added}$ is the added mass as a function of time [kg], $x$ is the horizontal displacement of the structure [m], $G$ is the dead load corrected for buoyancy [N], $\mu$ is the friction coefficient [-], and $g$ is the failure function for horizontal sliding [N].

Sliding of the structure occur when $g \leq 0$. The sliding distance ($x_2 - x_1$) is determined from the double time integration over the interval $t_1$ to $t_2$ in Eq. 6. $t_1$ is the instance where destabilizing forces are bigger than stabilizing forces and $t_2$ is the instance where the structure has come to rest. The sliding velocity, $u$, is calculated based on integration of the equation of motion and the static friction coefficient, $\mu_s$, and dynamic friction coefficient, $\mu_d$, is used when $u = 0$ and $|u| > 0$, respectively.

$$x(t_2) - x(t_1) = \int_{t_1}^{t_2}\int_{t_1}^{t} \frac{1}{M_{structure} + M_{added}} \cdot F(t)dtdt \qquad (6)$$

### Comparison of Measured and Calculated displacement

Measured and calculated sliding distances, using the simple one-dimensional approach in Eq. 6, are illustrated in Figure 12 *(right)* for the complete regular wave time-series and in Figure 12 *(left)* for the considered load peak. As seen, the simple approach clearly overestimates the sliding distance of the crown-wall, in contrast to the case for caisson breakwaters as observed by Burcharth et al. (2008) and Andersen et al. (2010). It should be mentioned, that the total calculated displacement in Figure 12 *(right)* is unrealistic and will lead to a complete failure of the structure. Moreover, despite the regular wave test case, some variability is observed in the calculated sliding distances for each wave in Figure 12 *(right)* which is believed to be due to reflections in the 2D flume.

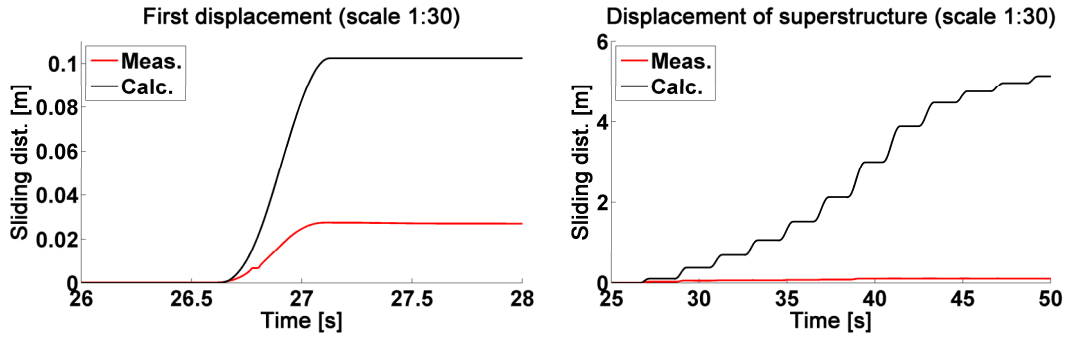


**Figure 12. *(left)* Measured and calculated sliding time-series of first wave load. *(right)* Measured and calculated total sliding time-series from regular waves.**

Three effects are expected to cause the overestimation of the sliding distance in Figure 12. The first effect may arise from rocking/tilting of the crown-wall or from influences of the elasticity in the

foundation. This effect will, however, be evaluated later using the more sophisticated two-dimensional Finite-Element model.

The second effect arises from the increasing crest width of the breakwater which causes a dampening effect on the wave loads after some sliding. This effect is clearly observed in Figure 12 *(right)* where the measured accumulated displacement stabilizes after some waves. According to Pedersen (1996), the influence from the crest width on the horizontal wave forces can be described by the ratio between the wave length of the mean wave period, $L_m$, and the crest width, $b$, $(L_m/b)^{0.5}$, indicating that an increasing crest width will lead to a reduced horizontal wave force on the superstructure. Thus, this wave length to crest width ratio should be taken into account when evaluating the backwards sliding of a crown-wall superstructure. The dampening effect is incorporated using the reduction factor, $\lambda_{sliding}$, in Eq. 7 for the total resulting wave load on the sliding section, cf. Eq. 8.

$$\lambda_{sliding} = \frac{\sqrt{L_m / \left(b_{initial} + \Delta b\right)}}{\sqrt{L_m / b_{initial}}} \quad , \quad \Delta b = b_{actual} - b_{initial}$$
$$\lambda_{sliding}\left(i\right) = \sqrt{\frac{b_{initial}}{b_{initial} + x\left(i\right)}} \tag{7}$$

where $b_{actual}$ is the accumulated crest width during sliding of the superstructure [m], $b_{initial}$ is the initial crest width [m], and $x(i)$ is the accumulated horizontal sliding distance at time instance $i$ [m].

$$F_{red} = \lambda_{sliding} \cdot F_{res} \tag{8}$$

where $F_{red}$ is the reduced resulting wave load on the structure [$kN$].

The influence from the accumulated sliding reduction factor $\lambda_{sliding}$ in Eq. 7 is illustrated in Figure 13. As seen, the calculated and measured sliding time-series stabilizes at the same level which indicates that the introduced sliding factor performs well. The first displacement is, however, still overestimated.

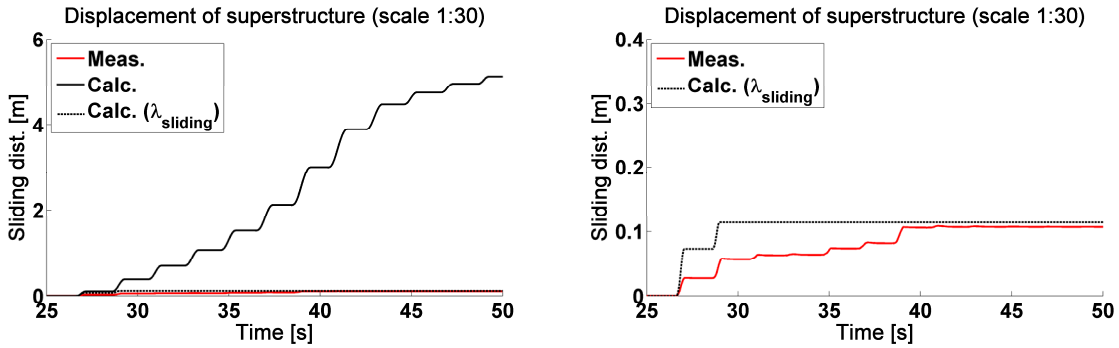


**Figure 13.** ***(left)*** **Measured and calculated total sliding distance time-series of the crown-wall with and without load reduction factor due increasing crest width.** ***(right)*** **Measured and calculated sliding distance time-series of first displacement of the crown-wall with and without load reduction factor due to increasing crest width.**

It should be mentioned, that the reduction factor in Eq. 7 is based on an unchanged crest height after displacement of the crown wall which is not always the case since the armor units can fall down when the wall slides backwards. This will leave the upper part of the crown wall unprotected. Some types of armor units are, however, interlocking, which leads to a remaining crest height after displacement.

The last effect arises from the reduced relative velocity of the wave and the moveable section compared to fixed structure which will reduce the wave loads on the moveable section compared to the fixed section and thereby cause an overestimation of the sliding distance when using the simple one-dimensional approach. A rough estimation of the load reduction factor is given in Eq. 9 based on the maximum particle velocity in the incident wave, $v_{particle,max}$, and the maximum sliding velocity of the crown-wall, $v_{wall,max}$.

$$v_{particle,\max} = 0.6 \ \ m/s, \ v_{wall,\max} = 0.1 \ \ m/s \qquad F_{H,reduction\ factor} = \frac{(0.6-0.1)^2}{0.6^2} = 0.694 \qquad (9)$$

The calculated reduction factor in the example in Eq. 9 is based on maximum velocities. Realistically, the reduction factor will be slightly higher due to smaller average relative velocity differences through the single displacement incident. In Figure 14 a reduction factor of 0.75 is used as an example which results in a good agreement between measured and calculated sliding distances and velocities. The reduction factor due to increasing crest width is further applied to the time-series in the figure. However, when solely evaluating the first movement of the structure in the time-series, and if only a small movement is obtained in the first wave incident, the effect from $\lambda_{sliding}$ is relatively small.

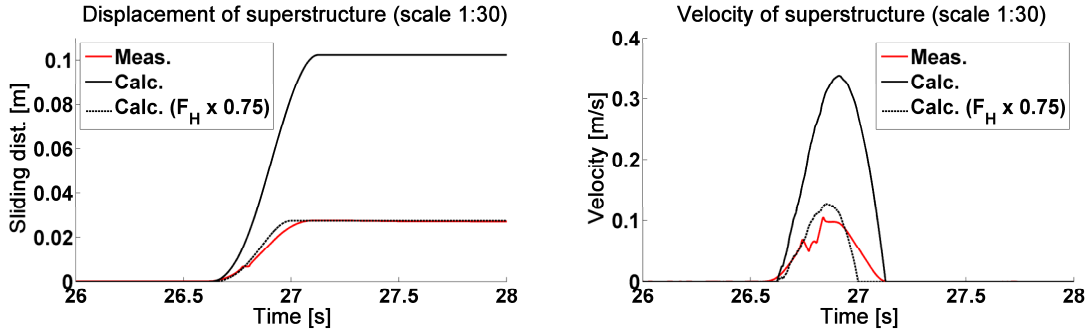


**Figure 14.** ***(left)*** **Measured and calculated sliding distance of crown-wall with and without load reduction factor due to decreased relative velocity.** ***(right)*** **Measured and calculated sliding velocity of crown-wall with and without load reduction factor due to decreased relative velocity and reduction factor due to increasing crest width.**

The actual load reduction should, however, be verified based on physical model tests where wave loads are measured on the moveable section instead of a fixed wall.

## NUMERICAL MODEL TEST STUDY

A more detailed analysis of the soil-structure interaction during wave impact on the crown-wall is obtained using the commercial Finite-Element code ABAQUS (Simulia. 2010). Plane strain is assumed in the ABAQUS model and fully drained behavior of the subsoil is assumed in order to reduce the computational effort to run the model. Four node quadrilateral elements with bilinear spatial interpolation of the displacement field are employed using so-called CPE4-elements which are available in ABAQUS with full integration of the stresses and mass. The sides of the soil domain are horizontally fixed, whereas the bottom is fully fixed. It is ensured that the soil domain is sufficiently large to avoid plastic strains near the edges. Moreover, it ensured that the reflected energy from the model boundaries is insignificant. The geometry and mesh are illustrated in Figure 15

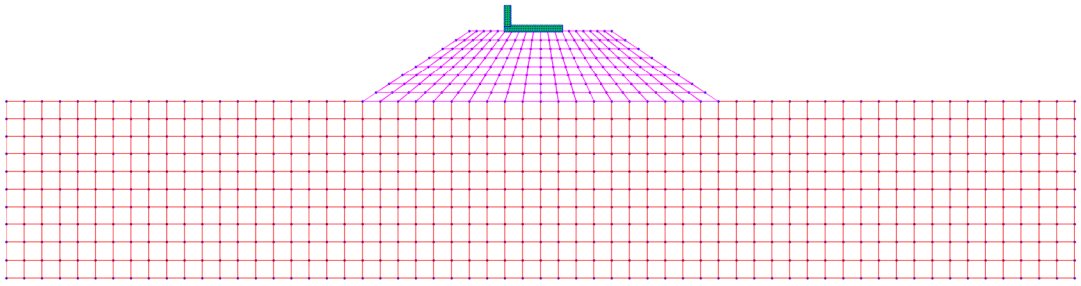

**Figure 15. Geometry and mesh applied in the ABAQUS model, generated in Matlab.**

The crown-wall is modelled as an impervious linear elastic isotropic material with the properties listed in Figure 16, where $E$ is the Young's modulus, $v$ is the Poisson's ratio, and $\rho$ is the mass density. The breakwater core material and seabed are consisting of quarry rock and sand, respectively. The breakwater armor layer is consisting of rock units and is included in the computational model by applying a corresponding pressure to the core material. The horizontal pressure from the armor layer on the crown-wall is not included in the computational model, which is also the case in the laboratory setup, cf. Figure 6 *(middle)*.

Below the soil material yield limit a linear elastic response is assumed, which is provided by the Mohr Coloumb criterion and based on the cohesion, $c$, and the friction angle, $\varphi$. Plastic deformations are included based on a non-associated plastic flow model which is described by the dilation angle, $\psi$. To increase the stability of the computational method, and to speed the computations, a cohesion of 1 *kPa* is introduced in the sand and the quarry material. Ideally, both materials should be modelled as non-cohesive materials, however, the influence of this artificial added cohesion on the results is believed to be insignificant.

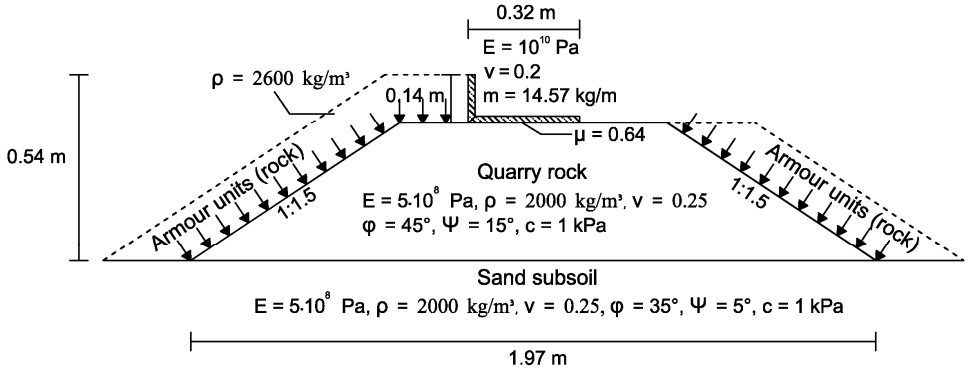


**Figure 16. Geometry of scale 1:30 ABAQUS model and material properties of the considered crown-wall, rubble-mound, and seabed**

Initial contact is assumed between the structure and foundation. However, slip is allowed during the dynamic response. A master-slave definition is employed in ABAQUS for the interface where the top of the core material is acting as a master surface and the base of the crown-wall is acting as slave. Wave loads on the crown-wall are applied in the ABAQUS model using a time discretization 0.004 s (250 Hz). Pressure is applied to each element in the crown-wall based on the interpolation of measured pressures from the applied pressure transducers in the laboratory tests cf. Figure 11.

**Numerical modeling of laboratory test setup (scale 1:30)**

Initially, the scaled laboratory setup is modelled in ABAQUS to evaluate the influence of the elastic response from the crown-wall foundation. This is followed by a model of the breakwater in prototype scale to evaluate sensitivity of the foundation elasticity and to evaluate possible scale effects arising from plastic strains in the core material in large scale which may not be present in small scale.

A comparison between the simple one-dimensional approach and the more sophisticated two-dimensional ABAQUS model is made in Figure 17. The density of the crown-wall material is specified to obtain the mass of the model in the laboratory. Additionally, the measured friction coefficient from the laboratory tests is specified in the ABAQUS model.

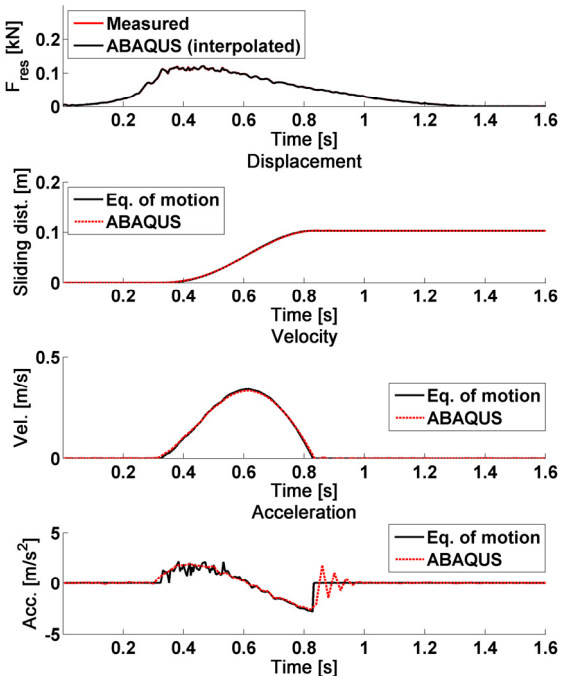


**Figure 17. Comparison between one-dimensional approach and the more sophisticated two-dimensional ABAQUS model**

As seen, a very good agreement is obtained between the two models, meaning that the displacement in the specific case can be sufficiently modelled using a one-dimensional model, i.e. rocking/tilting is not a part of the failure mode and elastic-plastic deformations in the soil is negligible. Some discrepancies between the two models are observed in the end of the acceleration time series due to the elastic response of the foundation, which however, appears not to have any effect on the horizontal sliding distance. As mentioned, the sensitivity of the influence from the foundation elasticity will be evaluated later.

### Numerical modeling of prototype scale (scale 1:1)

The soil characteristics in the crown-wall foundation are depending on the overlying pressure, and are thus impossible to scale correctly. It is therefore of high interest to determine whether any plastic deformations arise in the core material in prototype scale and whether this will affect the sliding distance of the crown wall. The prototype scale model is modelled using the geometry in Figure 18 with a material density of the crown-wall of $\rho = 2300$ kg/m$^3$, corresponding to reinforced concrete. The geometry of the crown wall superstructure in prototype scale have the dimensions sketched in Figure 18 with height $D = 4.2$ m and width $B = 9.6$ m.

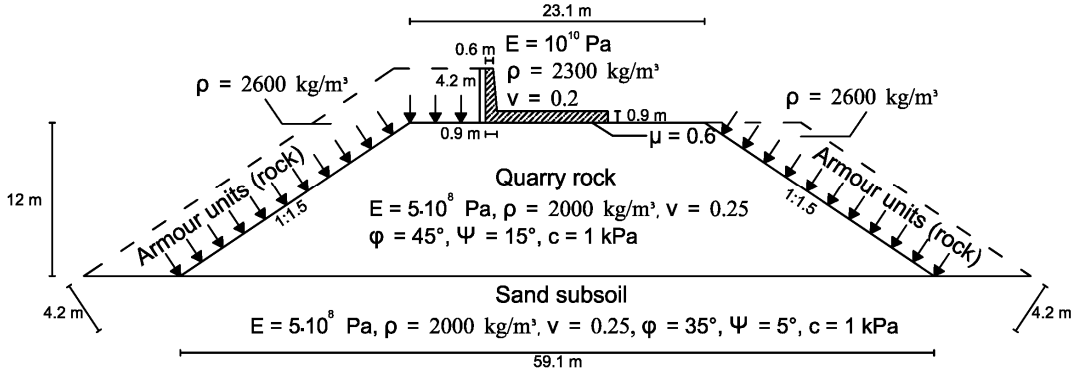


**Figure 18. Geometry of prototype scale ABAQUS model and material properties of the considered crown-wall, rubble-mound, and seabed**

Wave loads on the crown-wall are initially scaled using Froude's scaling law from scale 1:30 to scale 1:1. Hereafter, different load scales are applied to obtain different sliding distances to determine whether this can trigger any discrepancies between the one- and two-dimensional models. Results are given in Table 1 which indicates that only insignificant differences are obtained. It can thus be

concluded, that rocking/tilting has no influence on the accumulated displacement of the crown-wall superstructure in prototype scale either. Moreover, it is concluded that plastic failure in the underlying core material, which is not included in the simple one-dimensional model, has no influence on the sliding displacement of the crown wall.

**Table 1. Comparison of sliding distances (*D/B* = 0.438), scale 1:1**

| Load scale [-] | 1D-model [m] | Numerical model [m] | Difference [%] |
|---|---|---|---|
| 1.55 | 0.069 | 0.068 | 0.5 |
| 1.6 | 0.249 | 0.251 | -0.8 |
| 1.8 | 1.859 | 1.878 | -1.0 |
| 2 | 4.689 | 4.682 | 0.2 |
| 2.1 | 6.486 | 6.534 | -0.7 |

The elasticity of the quarry rock material in Figure 18 is chosen to have a typical value of $5 \cdot 10^8$ Pa. However, various elasticities are applied in the prototype-scale ABAQUS model to evaluate the sensitivity to the sliding displacement of the crown wall. A load scale of 1.6 is applied in the model to obtain sliding displacements which are sufficient for comparison. Results are given in Table 2 where it is seen, that the sliding displacement is influenced by the elasticity of the core material. A very stiff foundation material provides smaller displacements and vice versa. However, within realistic variations of $E$ ($3 \cdot 10^8$ Pa to $9 \cdot 10^8$ Pa) the difference between the sliding displacement from the one- and two-dimensional models is below 2%.

**Table 2. Sensitivity analysis on influence from stiffness of foundation (*D/B* = 0.438, load scale = 1.6), scale 1:1**

| E [Pa] | Relative E (E/ $5 \cdot 10^8$ Pa) [-] | 1D-model [m] | Numerical model [m] | Difference [%] |
|---|---|---|---|---|
| $9 \cdot 10^8$ | 1.80 | 0.249 | 0.248 | 0.4 |
| $7 \cdot 10^8$ | 1.40 | 0.249 | 0.250 | -0.4 |
| $5 \cdot 10^8$ | 1.00 | 0.249 | 0.251 | -0.8 |
| $3 \cdot 10^8$ | 0.60 | 0.249 | 0.253 | -1.6 |
| $1 \cdot 10^8$ | 0.20 | 0.249 | 0.261 | -4.6 |
| $5 \cdot 10^7$ | 0.10 | 0.249 | 0.281 | -11 |

Different crown-wall height/width ratios, *D/B*, are additionally evaluated to determine whether the rocking/tilting failure modes of the structure can become dominant for other geometries than the one tested in the laboratory tests. The different tested structure geometries in the given example are illustrated in Figure 19.

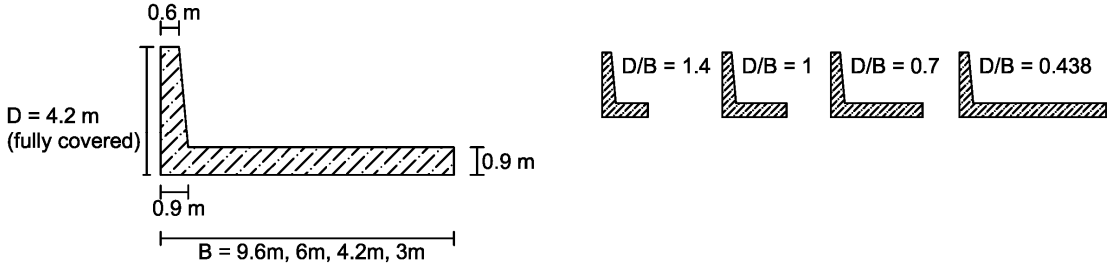


**Figure 19. Tested structure geometries with different height/width ratios.**

The smallest tested ratio, *D/B* = 0.438, is corresponding to the dimensions of the crown-wall evaluated in the laboratory tests, and the highest tested ratio is *D/B* = 1.4. Measured wave loads from the laboratory tests are applied to the different structure geometries, where the wave pressures on the structure geometries with higher *D/B*-ratios are cut-off corresponding to the illustration in Figure 20.

It should be mentioned, that the vertical pressure is more likely to be approaching zero at the rear corner of the base due to the relatively permeable core material. However, the cut-off pressure distribution in Figure 20 is chosen in order to have a comparable pressure distribution for the different considered *D/B*-ratios.

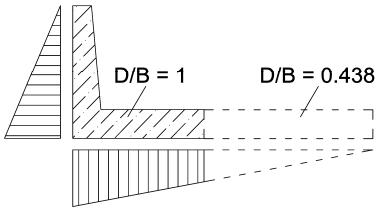


**Figure 20. Illustration of applied wave loads on the example crown-wall structures with different geometries than the geometry tested in the laboratory tests.**

A comparison between the sliding distances of the different height/width ratios from the one- and two-dimensional models is given in Table 3. Different load scale factors are applied to the different evaluated geometries to obtain sliding distances of approximately the same order. As seen, only small differences are obtained between the one- and two-dimensional models. The biggest difference is observed to be approximately 5 % but no clear tendency is observed from the different evaluated *D/B* ratios. It can thus be concluded, that despite the relatively narrow structure geometry of e.g. *D/B* = 1.4 horizontal sliding is still the most dominant failure mode and tilting has no influence on the horizontal displacement in the given case.

**Table 3. Sliding distances for various *D/B* ratios, scale 1:1**

| Load scale [-] | D/B [-] | 1D-model [m] | Numerical model [m] | Percentage diff. [%] |
|---|---|---|---|---|
| 1.6 | 0.438 | 0.249 | 0.251 | -0.8 |
| 1.25 | 0.7 | 0.221 | 0.228 | -3.0 |
| 1.115 | 1 | 0.248 | 0.260 | -4.8 |
| 1.02 | 1.4 | 0.169 | 0.168 | 0.4 |

Plastic strains from the ABAQUS model in scale 1:1 are illustrated in Figures 21 and 22 for the case with *D/B* = 0.438 resulting in a horizontal displacement of 0.251 m. As seen, only small plastic strains are observed directly under the crown-wall structure and no failure mechanism is arising in the remaining core material.

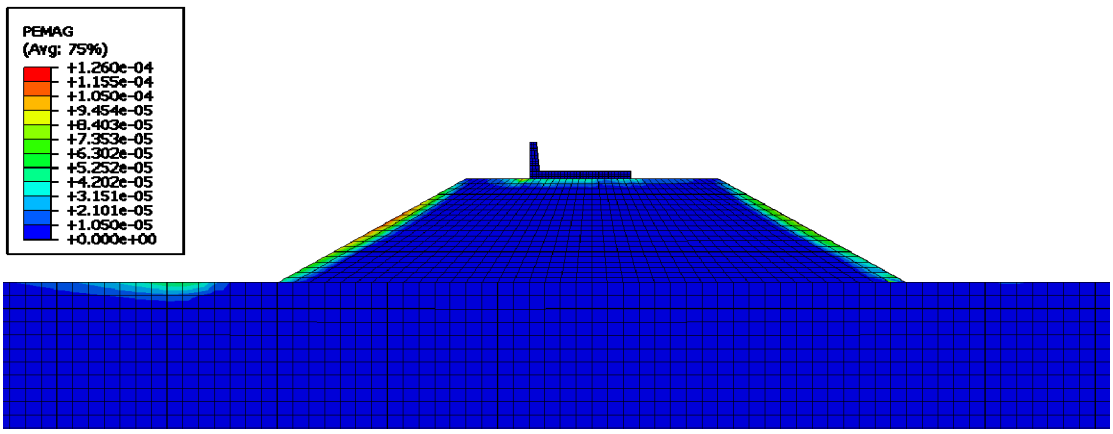


**Figure 21. Plastic strains for geometry with height/width ration of D/B = 0.438 in prototype scale 1:1.**

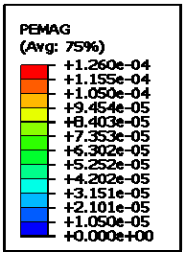

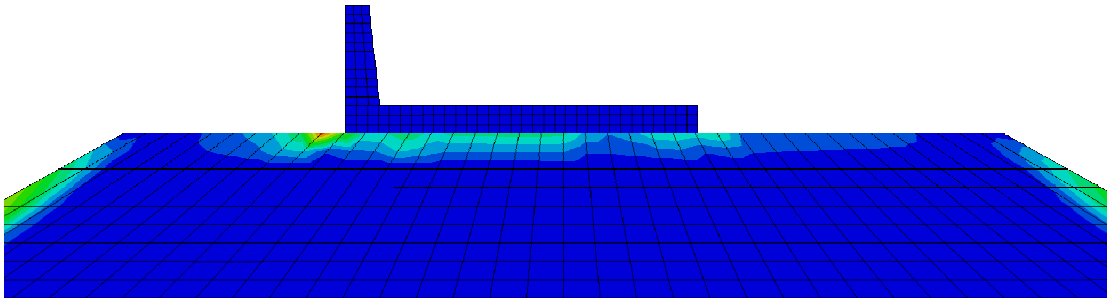

**Figure 22. Zoomed view of plastic strains for geometry with height/width ration of D/B = 0.438 in prototype scale 1:1.**

## CONCLUSIONS FROM PRESENT STUDY

Crown-wall superstructures are normally not designed to move during an extreme event with a given return period. However, the design sea state for existing structures is expected to change in the future due to climate changes leading to potential failures during extreme sea conditions. Instead of upgrading existing structures, which can be a very costly procedure, small movements of the structures could alternatively be accepted as long as total failure of the structure is not introduced. Such allowance, however, requires safe estimates of the structure displacements during a specific sea state and the present paper has evaluated different procedures of estimating these sliding distances.

An important finding in the present paper is that a simple one-dimensional model based on integration of the equation of motion with input from wave loads measured on a fixed structure provides a safe estimate of the sliding displacement of a typical crown-wall superstructure. This is in contrast to the case for caisson breakwaters as concluded in the research by Burcharth et al. (2008) and Andersen et al. (2010).

The wave loads on a sliding crown-wall superstructure are slightly reduced compared to the wave loads measured on a fixed structure due to accumulating increasing crest width when the structure slides backwards and due to the reduced relative velocity of the crown-wall and the maximum particle velocity in the incident wave. A sliding reduction factor for the influence from increasing breakwater crest is suggested in the present paper, inspired by Pedersen (1996), and based on the assumption of an unchanged crest height after displacement of the crown wall. Additionally, a roughly estimated reduction factor has been suggested to account for the reduced relative velocity of the crown-wall and wave particles. The suggested reduction factor is, however, based on an example case, and needs further investigation.

Wave loads on the crown-wall are concluded to be much less impulsive compared to wave loads on e.g. a caisson breakwater due to the protective effect of armour units. Both the vertical and horizontal pressure distribution is seen to be almost triangular which leads to a high stability against rocking and tilting of the structure. This high stability is further observed when comparing the simple one-dimensional sliding model with a more sophisticated two-dimensional Finite-Element model in scale 1:30 where identical horizontal sliding distances are obtained between the two models. Even for a relatively narrow geometry with a height/width ratio of 1.4 the structure is stable against overturning due to the non-impulsive nature of the wave loads.

The sophisticated Finite-Element model is further used to evaluate the influence from the elasticity of the breakwater core material and scale effects when converting from small scale to prototype scale without accounting for possible slip failure in the underlying foundation. From the numerical model it is concluded that within realistic variations of elasticity modules, the elasticity of the breakwater core material is of minor importance when evaluating the sliding displacement of the crown wall. Different sliding distances are triggered by applying different load scales, and only insignificant plastic failure is observed in the core material which has no influence on the displacement.

## SUGGESTED FUTURE STUDY AND FUTURE PERSPECTIVES

The load reduction factor arising from the decreased relative velocity of the wave particles and the crown-wall should be investigated further. This could be done by measuring wave loads directly on the moveable section and compare these with wave loads on the fixed structure. Such study should initially be performed on a vertical caisson instead of a crown wall to exclude the influence of the increasing crest width when the structure slides backwards.

The present study is solely based on long-crested regular waves. However, irregular waves can in some situations trigger more impulsive wave loads leading to slightly other conclusions than in the

present paper. Moreover, impulsive wave loads will arise if a part of the crown wall is left un protected by the armor units. The stability of the crown wall should be evaluated in such situations as well.

**ACKNOWLEDGEMENTS**

The support of the European Commission through FP7.2009-1, Contract 244104 - THESEUS ("Innovative technologies for safer European coasts in a changing climate"), is gratefully acknowledged.

**REFERENCES**

Andersen, L., Burcharth, H. F., & Lykke Andersen, T. (2010): *Validity of simplified Analysis of Stability of Caisson Breakwaters on Rubble Foundation Exposed to Impulsive Loads.* Proc. of the 32nd Int. Conf. on Coastal Eng.: Shanghai China.

Burcharth, H. F., Liu, Z., & Troch, P. (1999). *Scaling of Core Material in Rubble-mound Breakwater Model Tests.* Proc. of the Fifth International Conference on Coastal and Port Engineering in Developing Countries, Cape Town, South Africa(s. 1518-1528).

Burcharth, H. F., Andersen, L. & Lykke Andersen, T. (2008): *Analyses of Stability of Caisson Breakwaters on Rubble Foundation Exposed to Impulsive Loads.* Proc. of the 31st Int. Conf. on Coastal Eng.: Hamburg, Germany, pp. 3606-3618.

Pedersen, J. (1996). *Wave Forces and Overtopping on Crown-walls of Rubble-mound Breakwaters.* Ph.d. thesis, Aalborg University.

Simulia. 2010. *ABAQUS Version 6.10 Documentation*, Dassault Systèmes Simulia Corp., Providence, RI, USA.